Biochimica et Biophysica Acta 1838 (2014) 2412–2419

Contents lists available at ScienceDirect

Biochimica et Biophysica Acta

journal homepage: www.elsevier.com/locate/bbamem

Bilayer undulation dynamics in unilamellar phospholipid vesicles: Effect of temperature, cholesterol and trehalose

Beate-Annette Brüning [a,b,*], Sylvain Prévost [a], Ralf Stehle [a], Roland Steitz [a], Peter Falus [c], Bela Farago [c], Thomas Hellweg [d]

[a] Soft Matter and Functional Materials, Helmholtz-Zentrum Berlin, Hahn-Meitner Platz 1, 14109 Berlin, Germany
[b] Radiation Science and Technology, Delft University of Technology, Mekelweg 15, JB 2629 Delft, The Netherlands
[c] Time-of-Flight and High Resolution, Institut Laue Langevin, B. P. 156, 38042 Grenoble, Cedex 9, France
[d] Physical and Biophysical Chemistry, Bielefeld University, Universitätsstr. 25, 33615 Bielefeld, Germany

ARTICLE INFO

Article history:
Received 16 April 2014
Received in revised form 2 June 2014
Accepted 9 June 2014
Available online 17 June 2014

Keywords:
Vesicles
Fluctuations
Neutron spectroscopy

ABSTRACT

We report a combined dynamic light scattering (DLS) and neutron spin-echo (NSE) study on the local bilayer undulation dynamics of phospholipid vesicles composed of 1,2-dimyristoyl-glycero-3-phosphatidylcholine (DMPC) under the influence of temperature and the additives cholesterol and trehalose. The additives affect vesicle size and self-diffusion. Mechanical properties of the membrane and corresponding bilayer undulations are tuned by changing lipid headgroup or acyl chain properties through temperature or composition. On the local length scale, changes at the lipid headgroup influence the bilayer bending rigidity κ less than changes at the lipid acyl chain: We observe a bilayer softening around the main phase transition temperature T_m of the single lipid system, and stiffening when more cholesterol is added, in concordance with literature. Surprisingly, no effect on the mechanical properties of the vesicles is observed upon the addition of trehalose.

1. Introduction

In mammal organisms, lipid vesicles very often serve as natural carriers, for instance in the case of red blood cells or synaptic vesicles. Their functional properties strongly depend on the composition of their membranes [1–4]. In order to achieve valuable insight into that functionality, materials' properties such as the bending rigidity κ of the lipid membranes can be tuned by changes of temperature or composition. For the purpose, in this study we look at unilamellar vesicles (ULVs) of 1,2-di-myristoyl-glycero-3-phosphatidylcholine (DMPC) with the membrane additive cholesterol (Chol) or trehalose (Treh) added, (see Fig. 1). In the composite systems,the two additives can be considered complementary: due to its hydrophobic nature, cholesterol preferably arranges along the lipid acyl chains [4], whereas trehalose locates near the lipid headgroups [5]. An overview on how changes in temperature or amount of cholesterol or trehalose affect the membrane structure along the bilayer normal is given by Doxastakis et al. [6]. Temperature in fact plays an important role, in particular around the main phase transition. In single lipid systems, minor changes in temperature in close vicinity to the main phase transition temperature T_m produce a critical swelling of the lamellae associated with a lipid bilayer softening [7–10].

The co-surfactant cholesterol has been extensively studied with regard to its effects on bilayer self-assembly, phase state and structure [11–15], as well as on its mobility within the membrane [16,17]. Cholesterol inserts into the lipid bilayer membrane in concentrations of up to 50 mol% and is known to regulate membrane fluidity [18], permeability [19], rigidity [20–22] and the lateral mobility of proteins [23,24]. Its effect on membrane dynamics has been scrutinized over a broad range of time and length scales using quasi-elastic and inelastic scattering experiments [4,20–22,25,26]. The insertion of cholesterol into the lipid bilayer reduces free volume in the membrane plane, and thus influences collective in-plane dynamics [4,26].

The disaccharide trehalose has attracted comparable interest due to its bioprotective properties. Organisms that are able to survive potentially damaging conditions produce trehalose in high quantities during stress periods [27]. MD simulations predict that at low concentration trehalose stabilizes membrane structures by partially replacing water molecules in the hydration shell of the lipid headgroups via hydrogen bonding [6,27–29]. At high trehalose concentrations, the disaccharide can serve as a replacement for water under anhydrous conditions, which explains its effectiveness as lyophilization agent for vesicles and cells [28]. In the latter cases, the sugar molecules form a glassy state by interlinking different lipid headgroups, which prevents membrane fusion processes and reduces dehydration-induced stresses [30–34]. The MD simulations at low to moderate trehalose concentration (up to 30%) are in-line with experimental findings on the partitioning of trehalose into the headgroup region [5,35,36]. However, also partial

* Corresponding author at: Radiation Science and Technology, Delft University of Technology, Mekelweg 15, JB 2629 Delft, The Netherlands. Tel.: +31 15 278 1994.
E-mail address: B.A.Bruning@tudelft.nl (B.-A. Brüning).

http://dx.doi.org/10.1016/j.bbamem.2014.06.006
0005-2736/

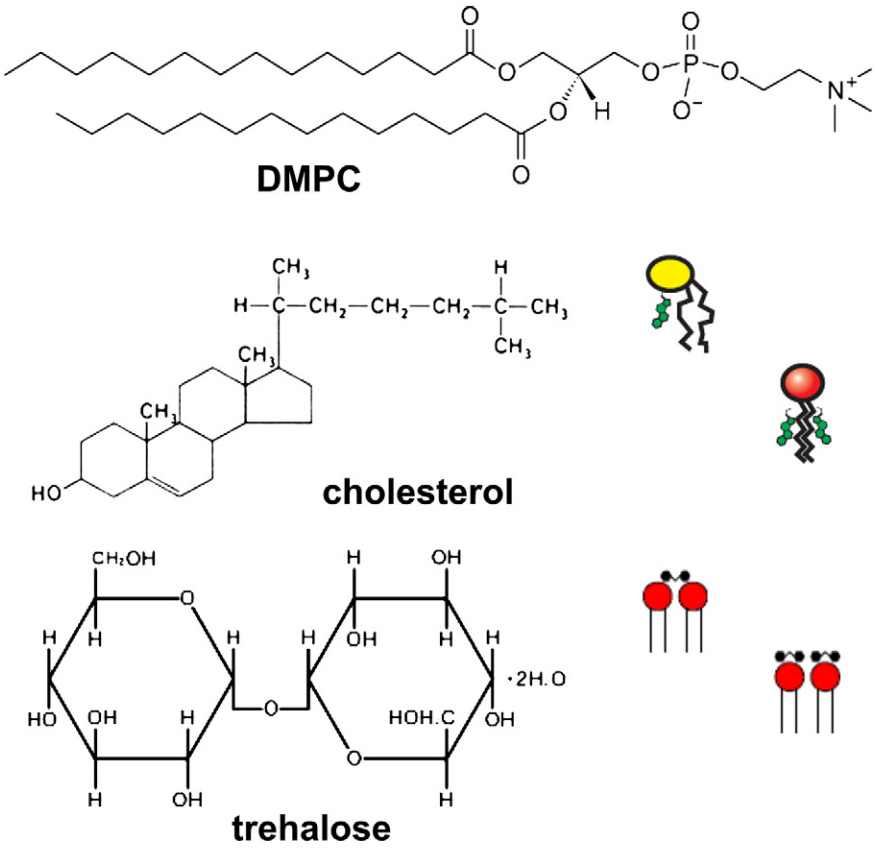

Fig. 1. Phospholipid molecule and membrane additives used in this study (*from top*): DMPC, cholesterol and trehalose. Due to its hydrophobic nature, cholesterol preferably locates near the DMPC acyl chain region, whereas trehalose attaches to the phospholipid headgroups (see schemes on the right of the respective structural formulae).

depletion of trehalose from the hydration layer was observed experimentally [37,38]. The concentration dependent change-over of membrane–sugar interactions, partitioning vs. depletion, was recently investigated by Andersen et al. [34]. The authors studied the interaction of trehalose with unilamellar vesicles of DMPC in D_2O by small-angle neutron scattering (SANS) and thermodynamic measurements. They observed strong binding of trehalose tothe interface, which made the membrane thinner and laterally more expanded at low trehalose concentration. Their experimental findings were confirmed by MD simulations by Kapla and co-workers who interpreted the experimental results as an intercalation effect of the trehalose molecules into the polar part of the lipids [39]. In the simulation, a decrease of lateral lipid mobility in the membrane plane was predicted in the presence of trehalose, as well as an increase in the bilayer bulk modulus.

The choice of appropriate means for the characterization of membrane mechanical properties such as bulk modulus and bending rigidity is strongly dependent on the system under investigation. In the case of giant unilamellar vesicles (GUVs) on the length scale of 10–50 μm, the membrane fluctuation dynamics is widely studied by optical and microscopy techniques [40–47]. Also dynamic light scattering (DLS) has occasionally been used [48].

X-ray and neutron diffraction techniques come into play whenever lipid systems get smaller and organized as multilamellar vesicles (MLVs). The elastic constants are obtained from the line shape analysis of the lipid bilayer Bragg peaks [49–51]. Neutron spin-echo [12,14] and MD simulations [13] further allow direct monitoring of membrane thickness fluctuations in that regime.

When it comes to unilamellar vesicles (ULVs) of the order of 50 nm in radius, which in a biological environment would correspond to sizes close to the ones of synaptic vesicles [52], long wavelength neutron spin-echo spectroscopy (NSE) is a well-suited experimental approach for a direct investigation of local lipid bilayer undulation dynamics and the membranes' corresponding mechanical properties. The ULVs we use are smaller than GUVs by three orders of magnitude and thus are subject to significantly different curvatures and interface line tensions.

In this work we use neutron spin-echo spectroscopy (NSE) to study the local lipid bilayer undulations and bending rigidities as a function of temperature or composition. We unfold the bilayer undulations and the vesicle center-of-mass diffusion by complementary dynamic light scattering (DLS) measurements and a combined analysis of NSE and DLS data [20,53,54]. Since cholesterol perturbs lipid bilayers non-universally, i.e. depending on lipid acyl chain saturation [40,55–57], we extend previous long wavelength NSE work by investigating how the sterol molecule affects the local undulations of lipid bilayers containing a fully saturated instead of a mono-unsaturated phospholipid. Moreover, a very interesting aspect to the topic is the influence of trehalose on bilayer undulations and bending rigidity directly.

2. Material and methods

2.1. Sample preparation

The lipids (DMPC, cholesterol) were purchased from Avanti (Alabaster, AL, USA) and dissolved in chloroform/trifluoroethanol (1:1) in the desired molar proportions. The solvent was subsequently evaporated slightly above room temperature in a vacuumoven and the dry lipids were hydrated with heavy water (D_2O) at a concentration of 10 mg/ml, heated from room temperature up to 30°C, ultrasonicated in a bath and cooled down to room temperature. This procedure was repeated three times. Trehalose was obtained from Merck (Darmstadt, Germany), dissolved in D_2O, and subsequently added to the dried phospholipid. In order to obtain unilamellar vesicles (ULVs), the suspension consisting of multilamellar vesicles (MLVs) was passed ten times through a polycarbonate filter with 50 nm pore diameter using

a LiposoFast Basic Extruder (Avestin, Canada), following the well-known extrusion method [58]. For the NSE experiments, the extruded phospholipid suspensions were poured into quartz cuvettes with a neutron pathway of 1 mm (Hellma, Müllheim, Germany). The cells had a quadratic cross section of 35 mm by 35 mm and were inserted into a designated thermostated sample holder.

2.2. Dynamic light scattering (DLS)

For the DLS measurements, an ALV goniometer with a 35 mW He–Ne laser operating at a wavelength of 632.8 nm was used with an ALV/High QE APD detector and an ALV-6010/160 external multiple τ digital correlator unit. The vesicle center-of-mass diffusion can be described by a correlation function $g_1(t) = exp(-D \cdot q^2 t)$, which is derived from the measured intensity correlation function $g_2(t)$ through the Siegert relation $g_1(t) = \sqrt{g_2(t)-1}$. The center-of-mass diffusion coefficient D and the hydrodynamic vesicle radius R_H are linked according to the Stokes–Einstein equation (Eq. (1)):

$$R_H = \frac{k_B T}{6\pi \cdot \eta(T) \cdot D}. \tag{1}$$

Here, D denotes the mean diffusion coefficient, k_B the Boltzmann constant, T the absolute temperature and $\eta(T)$ the temperature-dependent solvent viscosity (for D_2O at 30°C, $\eta(T) = 1.028 \cdot 10^{-3}$ Pa s). Our DLS measurements indicated that the averaged hydrodynamic radii R_H of the vesicles remained stable over the course of a week. The vesicles used for the NSE experiment were freshly prepared and measured within one day.

2.3. Neutron spin echo (NSE)

The method of neutron spin-echo spectroscopy (NSE) was first introduced by F. Mezei [59]. The local lipid bilayer undulation dynamics were investigated using the cold neutron spin-echo spectrometer IN15 at the Institut Laue Langevin (ILL, Grenoble, France). Nearly approaching the μs-regime, the instrument provides the longest Fourier times currently available on NSE-spectrometers. Due to its fine angular resolution in the small-angle regime (low q-values), the instrumentis well suited to probe the mesoscopic lengths scales often encountered in colloidal systems. The result of a measurement consists of a momentum transfer and time-resolved intermediate scattering function $S(q, t)$. The Fourier time t changes proportionally to the wavelength λ as well as to the applied magnetic field integral, following $t \propto \lambda^3 \int |B| dl$. Contrary to the correlation functions $g(t)$ measured by DLS, the q-interval probed by NSE lies in the range of the inverse length scales of local bilayer undulations. This allows a data interpretation on the basis of models including a unique q-dependence of the measured relaxation rates $\Gamma(q)$, such as the Zilman–Granek approach described in the theory section.

The IN15 instrument is situated at a cold polarizing neutron guide. Incident neutron wavelengths between 6 and 25 Å with a wavelength spread of 15% are available. At a distance of 4.6 m from the sample, the $^3He/CF_4$ multidetector is located, which covers 32 · 32 pixels of 1 cm^2 each. The detector center was moved to scattering angles of $2^\circ \le 2\theta \le 22^\circ$. Primary data corrections included correction with respect to instrumental resolution and empty cell plus solvent measurements. The instrumental resolution was determined by measuring graphoil as a purely coherent elastic scatterer. The correction was performed through division of sample scattering by the resolution signal [60].

3. Theory

Curvature free energy of elastic membranes is commonly expressed by the well-known Helfrich Hamiltonian [61]. Based on this continuum mechanical approach, Milner and Safran described the fluctuation dynamics of microemulsion droplets and vesicles [62]. In their theory, the normal bending modes of the flexible interface are coupled to the viscous friction exerted by the suspending medium with a single exponential decay $exp(-\Gamma_{MS} t)$ with a relaxation rate of $\Gamma_{MS} = \frac{\kappa}{4\eta} q^3$, where η is the effective viscosity of the solvent medium and κ the bending rigidity. In this manner, faster interfacial film relaxations are assigned to stiffer membranes. The momentum transfer q is related to the scattering angle 2θ between the incoming and final beam as $q = \frac{4\pi}{\lambda} \cdot sin\theta$. While well suited to describe data from soft interfaces, such as in microemulsion droplets and sponge phases, the expression fails to accurately account for the dynamics of phospholipid vesicles.

In a phenomenological approach, Zilman and Granek introduced a model to describe curvature shape fluctuations of freely suspended flat phospholipid bilayers [63,64]. On the local length scales probed by the NSE experiment, the lipid bilayer of a vesicle is approximately flat. The Zilman–Granek model takes into account a coupling of the bending modes and local diffusion processes: in a rigid membrane with a bilayer bending rigidity of $\kappa \gg k_B T$, less free volume can be explored by individual molecules; this means that the relaxation rate for a coupled process of undulation and local curvature will increase, whereas the average amplitude of the modes will decrease. The anomalous subdiffusive relaxation of the bending motions is described by a stretched exponential decay with a stretching exponent of $\beta = 2/3$:

$$\begin{aligned} S(q,t) &\propto exp(-\Gamma_u(q) \cdot t)^\beta \\ \text{with} \quad \Gamma_u(q) &= 0.025\gamma_q \left(\frac{k_B T}{\kappa}\right)^{1/2} \cdot \left(\frac{k_B T}{\eta(T)}\right) q^3 \end{aligned} \tag{2}$$

Within the relaxation rate $\Gamma_u(q)$, $\eta(T)$ denotes the temperature-dependent solvent viscosity. Further, γ_q is a weak monotonous function of the bending rigidity κ according to $\gamma_q = 1 - \frac{3}{4\pi}\left(\frac{k_B T}{\kappa}\right) \cdot ln(qh)$, where h is the membrane thickness, with $q \cdot h \approx 1$. For lipid model membranes, where κ lies on the order of several $k_B T$, γ_q can be approximated by unity [65]. In the following, we will discuss our data on the basis of the introduced model, comprising an additional term for the occurrence of underlying vesicle center-of-mass diffusion (Eq. (3)).

$$S(q,t)/S(q,0) = A \cdot exp(-\Gamma_d t) \cdot exp(-\Gamma_u t)^\beta \tag{3}$$

A is a normalization parameter close to one. The vesicle center-of-mass diffusion relaxation rate $\Gamma_d = D \cdot q^2$ is fixed to diffusion constants D obtained from dynamic light scattering. The relaxation rate of bilayer undulations Γ_u is a free parameter, while the stretched exponential is held fixed, following the Zilman–Granek approach. Note that the product of the two dynamic contributions in (q, t)-space corresponds to a mathematical convolution of two Lorentzians in (q, ω)-space commonly used in quasielastic neutron scattering experiments performed with other techniques, such as neutron backscattering or time-of-flight spectroscopy. With respect to previous work, such as e.g. [22], this seems to be a more general approach. However, comparing the outcome to the results obtained on the basis of the previously proposed description of the normalized intermediate scattering function $S(q, t)/S(q)$, we find that nosignificant differences are obtained within experimental precision.

4. Results

4.1. Dynamic light scattering (DLS)

DLS measurements were performed at scattering angles between 20° and 150° in steps of 10°. The obtained relaxation rates Γ_d vs. q^2 are shown for two exemplary samples in Fig. 2. A maximum error estimation amounts to up to five percent of the respective value [66]. Linear fits (solid lines) reveal a purely Fickian behavior typical of vesicle center-of-mass diffusion. The slope of these curves corresponds to the center-of-mass diffusion constant D, which clearly differs for pure

DMPC and DMPC/Trehalose (30 mol%). From the diffusion constant D, the hydrodynamic radii R_H shown in Fig. 3 are derived using the Stokes–Einstein relation (Eq. (1)).

For all investigated lipid mixtures, temperature ramps from 10°C to 60°C were done in steps of 5°C in both directions (up and down). Measurements were performed at a constant scattering angle. Diffusion constants were derived from CONTIN [67] and cumulant analysis [68] up to the third order. From the first and second order relaxation rates, a polydispersity index of around 0.15 was obtained for all extruded vesicles. For pure DMPC, the hydrodynamic vesicle radius R_H exhibits a pronounced temperature dependence around the main phase transition, as shown in (a): first a decrease in R_H occurs with rising temperature, culminating in an absolute minimum near $T_m = 23.6$°C. As the temperature is further increased, a slight increase in radius is observed, before it reaches a plateau value in the fluid phase. The temperature-dependence of R_H indicates that neither the number of lipids per vesicle northe number of vesicles remain constant. Thus, passing the main transition with rising temperature, the vesicles undergo lipid exchange and desorption processes. The nature of these exchange processes, which has been found to depend on lipid/solvent concentration, lipid chain length and phase state lies beyond the scope of this study. More information on the topic can be found e. g. in [69–71].

For the binary membranes, a qualitatively similar behavior is observed for the temperature dependence of the hydrodynamic radius R_H, which reaches a minimum near a reduced main transition temperature T_m. The temperature regime, in which thephase transition from gel to fluid phase occurs, broadens with increasing molar ratio of the membrane additive, cholesterol or trehalose (*not shown*). In terms of the phase transitions visible by dynamic light scattering, we have compared our data to published phase diagrams, [72]. The concentration dependence is obtained from the ramps for the different DMPC/cholesterol and DMPC/trehalose-ratios, and is shown in Fig. 3(b) and (c). In the following, mixing ratios of the composite systems are denoted in mol% of the membrane additive (cholesterol or trehalose, respectively). At a single lipid ratio and at constant temperature, the vesicles exhibit a reasonable stability within $\Delta R_H = \pm 2$ nm. The hydrodynamic radii R_H for pure DMPC and DMPC/Trehalose (30 mol%) do not inversely relate to the previously shown angle-dependent DLS results (Fig. 2). Thus, to estimate potential influences of the inter-vesicle structure factor or lipid exchange kinetics between the vesicles, exemplary samples were diluted down to 1 mg/ml concentration in D_2O solvent and remeasured. From the difference in the obtained hydrodynamic radii R_H, we estimate inter-vesicle interactions of up to ten percent within the momentum transfer range covered by DLS. This experimental result does not exceed an estimation based on the Carnahan–Starling equation [73]. Moreover, the momentum transfer ranges covered by DLS and NSE are well separated by several orders of magnitude due to the wavelength difference. The vesicle radius R_H shows a monotonous increase with rising amount of the additive, up to 30 mol% in case of Chol andup to 25 mol% in case of Treh, which suggests a homogenous mixture with the phospholipid membrane up to the investigated concentrations. For negligible changes in solvent viscosity, the center-of-mass diffusion constant D then scalesinversely with the amount of additive.

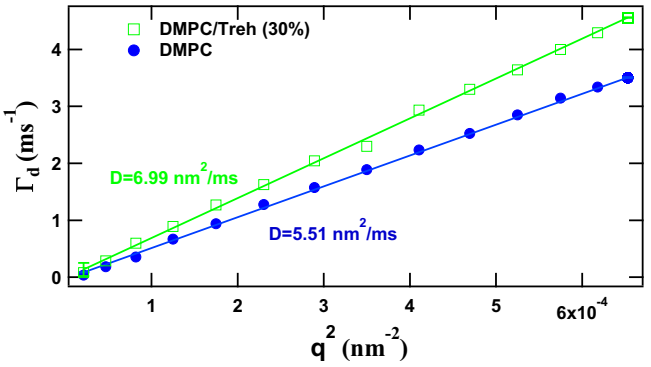

Fig. 2. Relaxation rate Γ_d vs. momentum transfer q^2, for DMPC and DMPC/trehalose vesicles (30 mol%, $T = 30$ °C). Solid lines represent linear fits, which yield the vesicle center-of-mass diffusion constant D. Error bars hardly exceed the symbol size.

4.2. Neutron spin echo (NSE): Bilayer undulations and vesicle center-of-mass diffusion

We now present our results on the local lipid bilayer undulation dynamics measured by NSE at neutron wavelengths of λ = 16 Å and

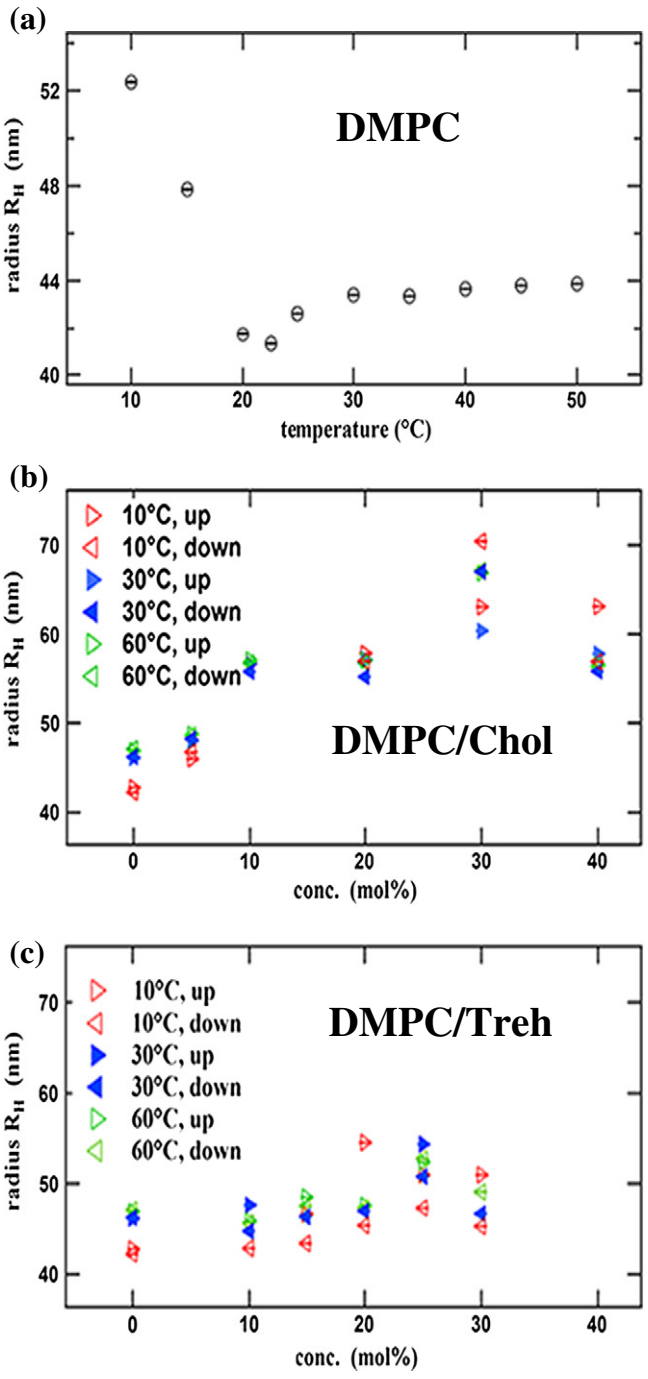

Fig. 3. Hydrodynamic vesicle radius R_H as obtained by dynamic light scattering (DLS): (a) DMPC for varying temperatures around main phase transition at $T_m = 23.6$ °C; (b) DMPC/cholesterol for varying molar ratios, ramping first up and thendown in temperature, and (c) DMPC/trehalose at varying molar ratios (analogous to (b)).

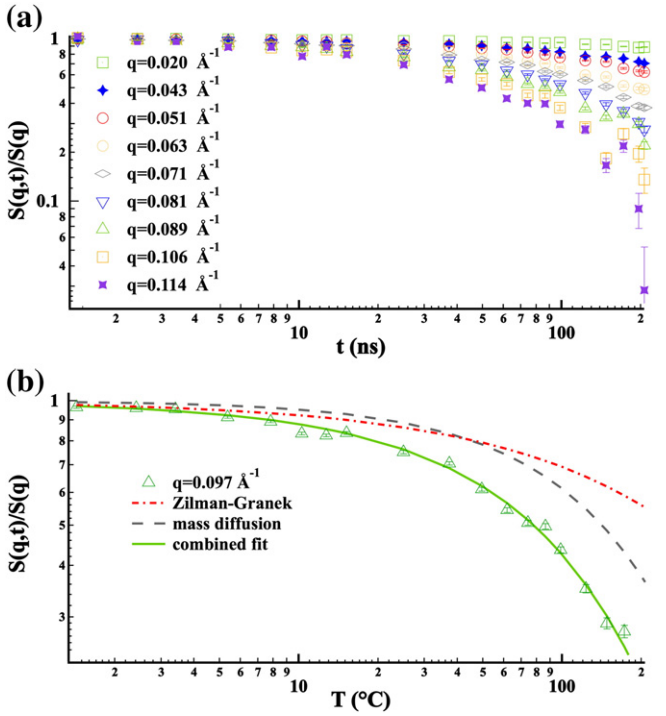

Fig. 4. Normalized intermediate scattering functions $S(q,t)/S(q)$ for DMPC standard at 30 °C: (a) whole q-range covered at $\lambda = 16$ Å; (b) combined fit according to Eq. (3), single contributions from vesiclecenter-of-mass diffusion and bilayer undulations.

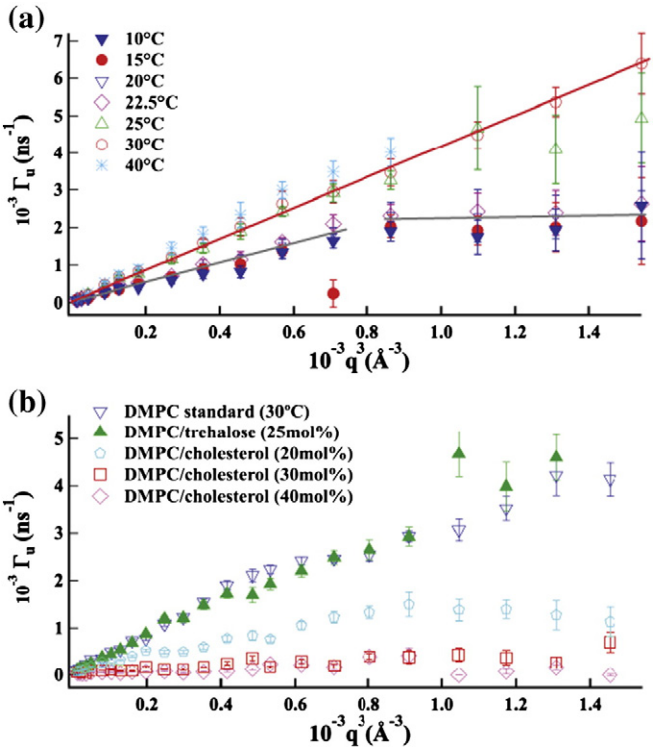

Fig. 5. Undulation relaxation rate $\Gamma_u(q^3)$: (a) temperature dependence around the main phase transition at $T_m = 23.6$ °C for pure DMPC; a deviation from a pure undulation mode is observed below the main transition at q-values above 0.8 (10^{-3}) Å^{-3}; and (b) effect of the respective membrane additives cholesterol and trehalose in composite lipid vesicles at 30 °C.

$\lambda = 17$ Å, respectively. The choice of these wavelengths in comparison to other NSE experiments wasbased on the necessity of measuring a full polarization decay within the probed (q, t)-window to separate dynamic contributions. In the supplementary information we show, that a full polarization decay is not obtained at a smaller wavelength of $\lambda = 10$ Å, which makes an unambiguous interpretation of the data difficult.

The normalized intermediate scattering function for our DMPC standard $S(q, t)/S(q)$ is shown for the long wavelengths and at varying q in Fig. 4(a). In order to remain within a stable fluid phase for all investigated lipid mixtures, NSE data were taken at 30°C. The covered Fourier times extend up to more than 200 ns, and the polarization nearly fully decays down to less than 0.1 at the largest momentum transfers q. At momentum transfers above $q = 0.071$ Å^{-1}, a distinct deviation from the single-exponential behavior is observed, starting at Fourier times between 40 and 100 ns (cf. supplementary information, Fig. 1). Moreover, we find that the fits can be improved taking into account dynamic contributions just outside the instrumental window in the μs-regime. Therefore, we take into account a vesicle center-of-mass diffusion contribution by inserting the diffusion constant D from DLS experiments into Eq. (3). In Fig. 4(b), both vesicle center-of-mass diffusion and bilayer undulation contributions are indicated separately for the pure DMPC standard for one exemplary q-value, as well as in a combined fit. On the double logarithmic scale the decay curvature is well matched by the fit at long Fourier times. By applying combined fits (Eq. (3)), the undulation relaxation rate $\Gamma_u(q^3)$ can thus be more clearly separated and analyzed.

We now look at the temperature dependence of the bilayer bending rigidity $\kappa(T)$ for the pure DMPC membrane, as derived from the linear slopes of the curves representing $\Gamma_u(q^3)$ (Fig. 5(a)). In particular, for the DMPC standard in its fluid phase (30° C), the result of $\kappa = 18.32 \pm 0.36\ k_BT$ derived from linear regression of $\Gamma_u(q^3)$ is well in accordance with literature values [74–76]. The inherent experimental error for κ is estimated to be on the order of k_BT. It corresponds to the

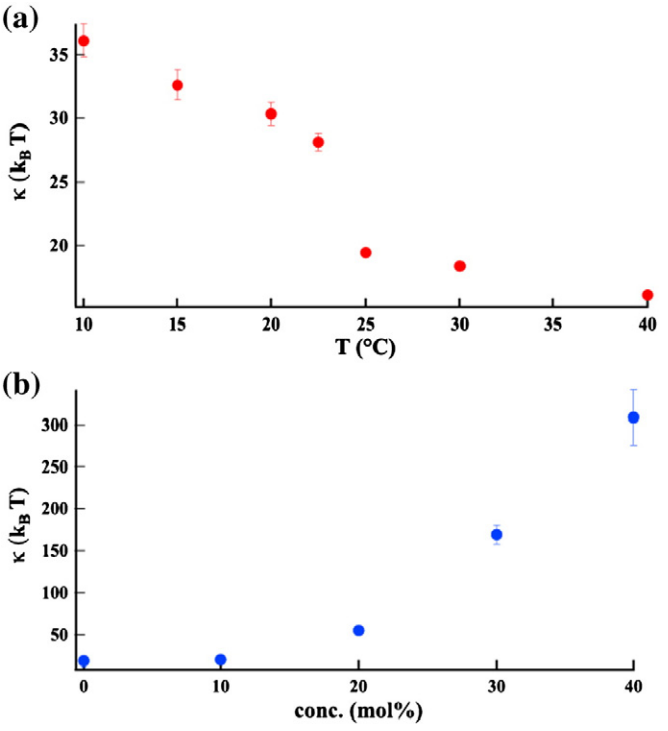

Fig. 6. Bilayer bending rigidity κ: (a) DMPC for varying temperatures: softening of the bilayer is observed near the main phase transition around $T_m = 23.6$ °C and above; and (b) DMPC/cholesterol: a distinct rigidification of the bilayer is observed with higher amounts of sterol at 30 °C.

difference in κ obtained for the DMPC standard during independent beam times [53,54]. The temperature dependence of the undulation relaxation rate $\Gamma_u(q^3)$ is shown in Fig. 5(a) for pure DMPC. The respective Fourier times were scaled following changes in the temperature induced D_2O solvent viscosity $\left(t \rightarrow t/\eta_{D_2O}(T)\right)$. In the fluid phase, above the main phase transition at $T_m = 23.6°$ C, the bilayer undulation relaxation rate $\Gamma_u(q^3)$ shows a linear dependence over the whole q-range measured. Slight increases in the linear slope indicate a minute softening (decrease of the bending rigidity κ) with increasing temperature. Below the main phase transition, an interesting observation can be made: $\Gamma_u(q^3)$ follows a linear slope up to $q_0^3 = 0.8$ Å^{-3}, before reaching a plateau at higher q^3-values. This saturation is most likely linked to the onset of combined curvature–compression modes introduced in an earlier contribution [25].

Overall, a softening of the bilayer membrane is observed with increasing T (Fig. 6(a)). This might be interpreted assuming a direct correlation between the free volume available to the lipid acyl chain segments in the membrane-plane and the bilayer bending rigidity κ: at the lowest measured temperature of 10°C, the lipid acyl chains are found in an *all-trans* conformation typical of the lipid's gel phase ($L_{\beta'}$). In this phase, the lipid molecules are packed most tightly in the membrane plane. The most prominent change occurs close to the main phase transition at $T_m = 23.6$°C between the ripple phase ($P_{\beta'}$) and the fluid phase (L_α). Here, the lipid acyl chains loose their characteristic *all-trans* conformation due to multiple gauche isomerizations. This loss in the acyl chain order leads to their effective shortening, as well as an increased demand in lateral space in the membrane plane and corresponding decrease in the lateral in-plane molecule density. As the main transition is cooperative and occurs at a defined temperature T_m, a distinct decrease in $\kappa(T)$ is visible. Further decrease with rising temperature might be linked to increased Brownian motions.

In a second step, the local bilayer undulation dynamics of the composite model membranes was investigated in an analogous manner, as shown for several exemplary compositions in Fig. 5(b). Insertion of rising amounts of cholesterol, clearly evokes a decrease in the slope of $\Gamma_u(q^3)$. For negligible changes in the solvent viscosity, this is an indication of a rigidification of the membrane (Eq. (2), Fig. 6(b)). We can explain the changes in the bilayer bending rigidity κ in a similar manner as for the temperature-dependence, since the largely hydrophobic cholesterol molecule mainly interacts with the lipid acyl chains. At low molar ratios, the weakly polar head of the sterol molecule forms hydrogen bridges with the polar lipid headgroups [77,78]. Due to this, the molecule arranges close to the already bulky phospholipid headgroups. Then, as only slight changes are induced in the lateral in-plane density, corresponding slight changes occur in the bending rigidity κ. At higher molar ratios, however, the sterol molecules require more space and inserts closer to the bilayer interior. In this process, the rigid sterol rings force the lipid acyl chains to straighten, which is often referred to as the 'condensing effect' of cholesterol on a membrane [77,79,80]. In this manner, the lateral in-plane molecule density increases in the acyl chain region, which is reflected in the observed increase in the bilayer bending rigidity κ (Fig. 6(b)).

Within experimental accuracy, the undulation relaxation rate $\Gamma_u(q^3)$ for 25 mol% trehalose closely resembles the one for the pure DMPC standard (Fig. 5(b), filled symbols), with the bilayer bending rigidity κ remaining unchanged under the influence of trehalose.

5. Discussion

The NSE data can be meaningfully analyzed, assuming a combination of two separable contributions within the probed dynamic window, namely vesicle center-of-mass diffusion and local lipid bilayer undulations. The latter contribution was described on the basis of the well-known Zilman–Granek approach for free film fluctuations.

For giant unilamellar vesicles (GUVs) of DMPC, the influence of temperature and varying cholesterol content on the bilayer bending rigidity κ was investigated by Meleard et al. using video microscopy [81]. In all cases, the reported bending rigidities κ for GUVs lie below the ones obtained in our case for ULVs. We attribute this to the difference in the respective vesicle radii for the two types of vesicles, which amounts to an order of magnitude. The smallervesicles in our case are non-equilibrium structures. They are subject to higher curvatures due to the extrusion process, which most likely provokes an additional line tension contribution at the membrane interface. As for the effect of increasing temperature, Meleard et al. obtain a bilayer bending rigidity κ, which remains more or less constant within the lipid's fluid phase between 26° and 40°C, in agreement with our findings. Using an all-optical method, Lee et al. have studied the temperature dependence of the bilayer bending rigidity $\kappa(T)$ of DPPC GUVs [82]. DPPC differs from DMPC by an extra CH_2 chain segment. Therefore, the main phase transition for DPPC occurs at higher temperatures. A drop in the bending rigidity $\kappa(T)$ of DPPC GUVs by an order of magnitude is found as the main phase transition is undergone, which is much more pronounced than the decrease that we obtain for the smaller DMPC vesicles. The main phase transition of small DPPC vesicles (20–40 nm) was studied in a recent simulation by Risselada and Marrink [83]. As the main transition from the gel to the fluid phase occurs, the authors observe a formation of gel domains in the bilayers, which could be effectively tuned by imposed area constraints. When comparing DMPC to DPPC vesicles, similar mechanisms are likely to play a role.

Cholesterol induced changes in the bilayer bending rigidity have already been reported by Arriaga et al. [20]. In fact, the results obtained for a POPC/cholesterol membrane and our current results for DMPC/cholesterol can be compared quantitatively, since we have performed both types of fits respectively consisting of a sum and of a product of exponential expressions to describe the two dynamic contributions. The resulting bending rigidities κ do not differ neither in magnitude nor in error bars between the two treatments (Fig. 6 in [20], Fig. 6(b)). Up to a sterol ratio of 10 mol%, the obtained bilayer bending rigidities κ agree quite well. At 20 mol%, however, we find DMPC/cholesterol to exhibit a greater stiffness than the POPC/cholesterol membrane. The difference between the two model membranes continuously increases with rising sterol ratio, until it reaches sixfold at 40 mol%. The deviation is likely to be explained by the single mono-unsaturated acyl chain of the POPC molecule, which in comparison to the fully saturated DMPC acyl chains partially diminishes the condensing effect of cholesterol on the membrane.

Our observation that trehalose leaves the bilayer bending rigidity κ largely unchanged up to 25 mol% is not easily explained, as neutron small-angle scattering reveals significant changes not only in the DMPC ULV membrane thickness (e. g. a decrease of 3.1 Å is observed at 20% trehalose), but also for DMPC MLVs a distinct increase in the intermembrane space of about 26 Å at 30% trehalose [36]. At least at length scales close to the membrane thickness, also the overall dynamics covered by neutron spin-echo spectroscopy should be influenced upon insertion of trehalose into the membranes, in concordance with the bilayer thickness fluctuations observed by Nagao for lamellar surfactant membranes [84]. However, due to the smaller q-range probed at long wavelengths, these fluctuations are only marginally covered and merely contribute to the error bars in our fits. In the past, it was also discussed in several studies, whether trehalose preferably interacts with the lipid headgroups and neighboring bound water, or with the surrounding bulk water: Winther et al. investigated the hydration and mobility of trehalose in aqueous solution and distinguished between two models of first and second order dynamic couplings between sugar and solvent [85]. In their work, the authors explicitly rule out clustering effects of trehalose molecules in water. However, in a recent neutron diffraction study Kent et al. find that at the physiologically relevant trehalose concentrations we also look at, the sugar molecules show no preference for localizing near the lipid headgroups [86]. Since trehalose at the given concentration induces merely small changes in the viscosity of the D_2O-solvent [87], the bilayer undulations probed

by NSE would then appear similar to that of the pure DMPC-vesicles. Thus, our results also support the view that the bioprotective effects of trehalose are caused by non-specific mechanisms that are not linked to changes directly at the membrane/water interface.

6. Conclusions

We have investigated the effect of temperature and the effects of the membrane additives cholesterol and trehalose on DMPC vesicles, in view of characteristic bilayer undulations and bending rigidity κ. Effects on vesicle morphology, vesicle size and self-diffusion, as well as shifts in the membrane phase state were also examined. We find that on the local length scale changes at the lipid headgroup influence the interfaces and bilayer bending rigidity κ less than at the lipid acyl chain: We observe a bilayer softening around the main phase transition temperature T_m of the single lipid system, and a bilayer stiffening with increasing cholesterol concentration in the binary mixture. The addition of trehalose, on the contrary, does not change interface undulations and bending rigidity κ at all. In summary, a picture emerges that lipid bilayer undulation dynamics and corresponding bending rigidities κ can be most aimfully tuned by directly inducing changes in the free volume within the acyl chain region of the membrane: the insertion of cholesterol, which partitions in the membrane near the lipid acyl chains, reduces the available free volume, thus an increase in the bilayer bending rigidity κ is observed. Consequently, it can be understood why adding trehalose has little effect on the local lipid bilayer undulation dynamics. The disaccharide binds to the already tightly packed phospholipid headgroups, thereby evoking little change in the free volume occupied by the lipid chains. Our findings suggest that changes invoked at the lipid acyl chains outweigh previously reported water replacement through trehalose or that changes directly at the membrane/water interface seem not to be induced at physiological sugar concentrations.

Acknowledgments

We thank K. Henziger and R. Köhler for the experimental support during the spin-echo beam times at ILL, and C. Schneider for providing the dynamic light scattering setup at HZB. We acknowledge HZB for the financial support and the ILL for the allocation of beam time on IN15, as well as for technical support.

Appendix A. Supplementary data

Supplementary data to this article can be found online at http://dx.doi.org/10.1016/j.bbamem.2014.06.006.

References

[1] P.-J. Chen, Y. Liu, T.M. Weiss, H.W. Huang, H. Sinn, E.E. Alp, A. Alatas, A. Said, S.-H. Chen, Biophys. Chem. 105 (2003) 721–741.
[2] J. Hub, T. Salditt, M.C. Rheinstädter, B.L. de Groot, Biophys. J. 93 (2007) 3156–3168.
[3] M.C. Rheinstädter, J. Das, E.J. Flenner, B. Brüning, T. Seydel, I. Kosztin, Phys. Rev. Lett. 101 (2008) 248106.
[4] B. Brüning, M.C. Rheinstädter, A. Hiess, B. Weinhausen, T. Reusch, S. Aeffner, T. Salditt, Eur. Phys. J. E. 31 (2010) 419–428.
[5] M. Luzardo, F. Amalfa, A.M. Nunez, S. Diaz, A.C. Biondi de Lopez, E.A. Disalyo, Biophys. J. 78 (2000) 2452–2458.
[6] M. Doxastakis, A.K. Sum, J.J. de Pablo, J. Phys. Chem. B 109 (2005) 24173–24181.
[7] R. Zhang, W. Sun, S. Tristam-Nagle, R.L. Headrick, R.M. Suter, J.F. Nagle, Phys. Rev. Lett. 74 (1995) 2832–2835.
[8] J.F. Nagle, H.I. Petrache, N. Gouliaev, S. Tristam-Nagle, Y. Liu, R.M. Suter, K. Gawrisch, Phys. Rev. E. 58 (1998) 7769–7776.
[9] G. Pabst, H. Amenitsch, D.P. Kharakoz, P. Laggner, M. Rappolt, Phys. Rev. E. 70 (2004) 021908.
[10] N. Chu, N. Kucerka, Y. Liu, S. Tristam-Nagle, J.F. Nagle, Phys. Rev. E. 71 (2005) 041904.
[11] T.A. Harroun, J. Katsaras, S.R. Wassall, Biochemistry 45 (2006) 1227–1233.
[12] T.A. Harroun, J. Katsaras, S.R. Wassall, Biochemistry 47 (2008) 7090–7096.
[13] W. Schrader, R. Behrends, U. Kaatze, J. Phys. Chem. B 116 (2012) 2446–2454.
[14] N. Kucerka, J. Pencer, M.-P. Nieh, J. Katsaras, Eur. Phys. J. E. 23 (2007) 247–254.
[15] L.X. Finegold, Cholesterol in membrane models, CRC Press, New York, 1992.
[16] C. Gliss, O. Randel, H. Casalta, E. Sackmann, R. Zorn, T. Bayerl, Biophys. J. 77 (1999) 331–340.
[17] S. Garg, L. Porcar, A.C. Woodka, P.D. Butler, U. Perez-Salas, Biophys. J. 101 (2011) 370–377.
[18] O.G. Mouritsen, K. Jorgensen, Chem. Phys. Lipids 73 (1994) 3–25.
[19] J.C. Mathai, S. Tristam-Nagle, J.F. Nagle, M.L. Zeidel, J. Gen. Physiol. 131 (2008) 69–76.
[20] L.R. Arriaga, I. Lopez-Montero, F. Monroy, G. Orts-Gil, B. Farago, T. Hellweg, Biophys. J. 96 (2009) 3629–3637.
[21] M.F. Hildenbrand, T.M. Bayerl, Biophys. J. 88 (2005) 3360–3367.
[22] L.R. Arriaga, I. Lopez-Montero, G. Orts-Gil, B. Farago, T. Hellweg, F. Monroy, Phys. Rev. E. 80 (2009) 031908.
[23] J.R. Silvius, Biochim. Biophys. Acta 1610 (2003) 174–183.
[24] P.L. Chong, W. Zhu, B. Venegas, Biochim. Biophys. Acta 1788 (2009) 2–11.
[25] L.R. Arriaga, R. Rodriguez-Garcia, I. Lopez-Montero, B. Farago, T. Hellweg, F. Monroy, Eur. Phys. J. E. 31 (2010) 105–113.
[26] S. Busch, T. Unruh, Biochim. Biophys. Acta 1808 (2010) 199–208.
[27] C.S. Pereira, R.D. Lins, I. Chandraskhar, L.C.G. Freitas, P.H. Hünenberger, Biophys. J. 86 (2004) 2273–2285.
[28] A.K. Sum, R. Faller, J.J. de Pablo, Biophys. J. 85 (2003) 2830–2844.
[29] M.A. Villarreal, S.B. Diaz, E.A. Disalvo, G.G. Montich, Langmuir 20 (2004) 7844–7851.
[30] L.M. Crowe, D.S. Reid, J.H. Crowe, Biophys. J. 71 (1996) 2087–2093.
[31] J.H. Crowe, J.F. Carpenter, L.M. Crowe, Annu. Rev. Physiol. 60 (1998) 73–103.
[32] K.L. Koster, Y.P. Lei, M. Anderson, S. Martin, G. Bryant, Biophys. J. 78 (2000) 1932–1946.
[33] S. Ohtake, C. Schebor, J.J. de Pablo, Biochim. Biophys. Acta 1758 (2006) 65–73.
[34] H.D. Anderson, C. Wang, L. Arleth, G.H. Peters, P. Westh, PNAS 108 (2011) 1874–1878.
[35] C. Lambruschini, A. Relini, A. Ridi, L. Cordone, A. Gliozzi, Langmuir 16 (2000) 5467–5470.
[36] M.A. Kiselev, J. Zbytovska, D. Matveev, S. Wartewig, I.V. Gapienko, J. Perez, P. Lesieur, A. Hoell, R. Neubert, Colloids Surf. B 256 (2005) 1–7.
[37] T. Söderlund, J.-M.I. Alakoskela, A.L. Pakkanen, P.K.J. Kinnunen, Biophys. J. 85 (2003) 2333–2341.
[38] P. Westh, Phys. Chem. Chem. Phys. 10 (2008) 4110–4112.
[39] J. Kapla, J. Wohlert, B. Stevensson, O. Engstrom, G. Widmalm, A. Maliniak, J. Phys. Chem. B 22 (2013) 6667–6673.
[40] R.S. Gracia, N. Bezlyepkina, R.L. Knorr, R. Lipowsky, R. Dimova, Soft Matter 6 (2010) 1472–1482.
[41] E. Evans, W. Rawicz, Phys. Rev. Lett. 64 (1990) 2094–2097.
[42] H.P. Duwe, J. Kaes, E. Sackmann, J. Phys. Fr. 51 (1990) 945–962.
[43] J. Käs, E. Sackmann, Biophys. J. 60 (1991) 825–844.
[44] R. Dimova, B. Pouligny, C. Dietrich, Biophys. J. 79 (2000) 340–356.
[45] J. Henriksen, A.C. Rowat, J.H. Ipsen, Eur. Biophys. J. 33 (2004) 732–741.
[46] J. Genova, A. Zheliaskova, M.D. Mitov, J. Optoelectron. Adv. Mater. 9 (2007) 427–430.
[47] P. Meleard, T. Pott, Adv. Planar Lipid Bilayers Liposomes 1 (2013) 55–75.
[48] P. Brocca, L. Cantu, M. Corti, E. Del Favero, S. Motta, Langmuir 20 (2004) 2141–2148.
[49] C.R. Safinya, D. Roux, G.S. Smith, S.K. Sinha, P. Dimon, N.A. Clark, A.M. Bellocq, Phys. Rev. Lett. 57 (1986) 2718–2721.
[50] G. Pabst, M. Rappolt, H. Amenitsch, P. Laggner, Phys. Rev. E. 62 (2000) 4000–4009.
[51] F. Nallet, R. Laversanne, D. Roux, J. Phys. II Fr. 3 (1993) 487–502.
[52] S. Castorph, S. Schwarz Henriques, M. Holt, D. Riedel, R. Jahn, T. Salditt, Eur. Phys. J. E. 34 (2011) 63.
[53] B. Brüning, R. Stehle, P. Falus, B. Farago, Eur. Phys. J. E. 36 (2013) 77.
[54] B. Brüning, B. Farago, Phys. Rev. E. 89 (2014) 040702(R).
[55] J. Pan, T.T. Mills, S. Tristam-Nagle, J.F. Nagle, Phys. Rev. Lett. 100 (2008) 198103.
[56] J. Pan, S. Tristam-Nagle, J.F. Nagle, Phys. Rev. E. 80 (2009) 021931.
[57] G. Khelashvili, N. Johner, G. Zhao, D. Harries, H.L. Scott, Chem. Phys. Lipids 178 (2014) 18–26.
[58] L.D. Mayer, M.J. Hope, R.P. Cullis, Biochim. Biophys. Acta 858 (1986) 161–168.
[59] F. Mezei, C. Pappas, T. Gutberlet (Eds.), Neutron spin echo spectroscopy, Springer, Berlin, 2003.
[60] B. Farago, Curr. Opin. Colloid Interface Sci. 14 (2009) 391–395.
[61] W. Helfrich, Z. Naturforsch. C 28 (1973) 693–703.
[62] S.T. Milner, S.A. Safran, Phys. Rev. A 36 (1987) 4371–4379.
[63] A.G. Zilman, R. Granek, Phys. Rev. Lett. 77 (1996) 4788–4791.
[64] A.G. Zilman, R. Granek, Chem. Phys. 284 (2002) 195–204.
[65] M. Klostermann, R. Strey, T. Sottmann, R. Schweins, P. Lindner, O. Holderer, M. Monkenbusch, D. Richter, Soft Matter 8 (2012) 797–807.
[66] T. Hellweg, Makromolekulare Strukturen in einem anderen Licht—Anwendungen der quasielastischen Lichtstreuung, Cuvillier, Göttingen, 1996.
[67] S.W. Provencher, Comput. Phys. Commun. 27 (1982) 213–227.
[68] D.E. Koppel, J. Chem. Phys. 57 (1972) 4814.
[69] J.D. Jones, T.E. Thompson, Biochemistry 28 (1989) 129–134.
[70] J.D. Jones, T.E. Thompson, Biochemistry 29 (1990) 1593–1600.
[71] W.C. Wimley, T.E. Thompson, Biochemistry 30 (1991) 1702–1709.
[72] P.F.F. Almeida, W.L.C. Vaz, T.E. Thompson, Biochemistry 31 (1992) 6739–6747.
[73] Norman F. Carnahan, Kenneth E. Starling, J. Chem. Phys. 51 (1969) 635.
[74] K.R. Mecke, T. Charitat, F. Graner, Langmuir 19 (2003) 2080–2087.
[75] M.C. Rheinstädter, W. Häußler, T. Salditt, Phys. Rev. Lett. 97 (2006) 048103.
[76] C.R. Safinya, D. Roux, G.S. Smith, S.K. Sinha, P. Dimon, N.A. Clark, A.M. Bellocq, Phys. Rev. Lett. 57 (1989) 2718–2721.
[77] J. Huang, G.W. Feigenson, Biophys. J. 76 (1999) 2142–2157.
[78] F. Richter, G. Rapp, L. Finegold, Phys. Rev. E. 63 (2001) 051914.
[79] F.J.-M. de Meyer, A. Benjamini, J.M. Rodgers, Y. Misteli, B. Smit, J. Phys. Chem. B 114 (2010) 10451–10461.

[80] W.-C. Hung, M.-T. Lee, F.-Y. Chen, H.W. Huang, Biophys. J. 92 (2007) 3960–3967.
[81] P. Meleard, C. Gerbeaud, T. Pott, L. Fernandez-Puente, I. Bivas, M.D. Mitov, J. Dufourcq, P. Bothorel, Biophys. J. 72 (1997) 2616–2629.
[82] C.-H. Lee, W.-C. Lin, J. Wang, Phys. Rev. E. 64 (2001) 020901(R).
[83] H. Jelger Risselada, S.J. Marrink, Soft Matter 5 (2009) 4531–4541.
[84] M. Nagao, Phys. Rev. E. 80 (2009) 031606.
[85] L.R. Winther, J. Qvist, B. Halle, J. Phys. Chem. B 116 (2012) 9196–9207.
[86] B. Kent, T. Hunt, T.A. Darwish, T. Hau, C.J. Garvey, G. Bryant, J. R. Soc. Interface 95 (2014) 20140069.
[87] T. Uchida, M. Nagayama, K. Gohara, J. Cryst. Growth 311 (2009) 4747–4752.